Polym. Bull. (2018) 75:1211–1235
https://doi.org/10.1007/s00289-017-2088-x

ORIGINAL PAPER

Transparent sulfur-containing thermoplastic polyurethanes with polyether and polycarbonate soft segments

Magdalena Rogulska[1]

Received: 16 February 2017 / Revised: 25 May 2017 / Accepted: 5 June 2017 /
Published online: 9 June 2017

Abstract New thermoplastic polyether- and polycarbonate-based segmented polyurethanes were synthesized by a catalyzed one-step melt polyaddition from diphenyl sulfide-derivative diol, i.e., 2,2′-[sulfanediylbis(benzene-1,4-diyloxy)]diethanol as a nonconventional chain extender, 1,1′-methanediylbis(4-isocyanatocyclohexane), and 40, 50, and 60 mol% poly(hexane-1,6-diyl carbonate) diol (PHCD) of $\overline{M}_n = 860$ g/mol or poly(oxytetramethylene) diol (PTMO) of $\overline{M}_n = 1000$g/mol as soft segments. The structures and thermal properties of the polymers were examined by FTIR, elemental analysis, differential scanning calorimetry, thermogravimetry (TG), and TG-FTIR. Moreover, their Shore A/D hardness, tensile, physicochemical, adhesive, and optical properties were determined. The obtained colorless, transparent, amorphous materials exhibited elastomeric or plastic properties. The PTMO-based polymers showed lower glass-transition temperatures than those based on PHCD (from −29 to 5 °C vs. from 11 to 43 °C) as well as a higher degree of microphase separation. On the other hand, the polymers with the polycarbonate soft segments revealed better transparency (transmittance at 800 nm: 84–89% vs. 75–82%), higher tensile strength (up to 48.6 MPa vs. up to 28.3 MPa), and hardness in comparison with those with the polyether soft segments. The polymers decomposed in two (in helium) or three (in air) stages and possessed a relatively good thermal stability. Their temperatures of 1% mass loss were contained within the range of 255–274 °C. In inert atmosphere, the values shown by polymers from PTMO were higher than those from PHCD, whereas in oxidative atmosphere, the situation was reversed. The newly synthesized sulfur-containing polymers showed a higher refractive index and adhesive strength to copper than analogous polymers based on butane-1,4-diol as a chain extender.

✉ Magdalena Rogulska
mrogulska@umcs.lublin.pl

[1] Department of Polymer Chemistry, Faculty of Chemistry, Maria Curie-Skłodowska University, ul. Gliniana 33, 20-614 Lublin, Poland

Keywords Sulfur-containing polyurethanes · Aliphatic–aromatic chain extender · HMDI · Polycarbonate and polyether soft segments · Thermal and mechanical properties · Adhesive and optical properties

Introduction

Thermoplastic polyurethane elastomers (TPUs) have an important place in the global production of polymeric materials. They are currently widely employed in medicine, footwear, automobile industry, etc. [1–3]. Their popularity derives from the fact that their functional properties, e.g., mechanical strength, elasticity, chemical and light resistance, and transparency, can easily be varied by the choice of their structural units and preparation conditions. TPUs are multiblock copolymers, often called segmented, whose macromolecules are made of alternately distributed hard segments constructed of diisocyanate and short-chain diols (chain extenders), and soft segments formed by long-chain diols such as polyether, polyester, or polycarbonate diols. The hard segments bear a strong influence on the modulus, hardness, and tear strength, while the soft segments impart softness, elasticity, long elongation at break and low-temperature resistance. TPUs with hard segments produced from 1,1′-methanediylbis(4-isocyanatobenzene) and butane-1,4-diol (BD) generally possess superior mechanical properties [3], but as aromatic diisocyanate are used, they tend to yellow upon exposure to ultraviolet and visible light as well as heat; that may lead even to their total destruction [2–7]. These drawbacks are restrictions to the expansion of their applications in high-quality materials and outdoor functions. Enhanced yellowing resistance is exhibited by polymers derived from aliphatic diisocyanates, e.g., 1,1′-methanediylbis(4-isocyanatocyclohexane) (HMDI), 1,6-diisocyanatohexane, and 5-isocyanato-1-(isocyanatomethyl)-1,3,3-trimethylcyclohexane [8]. Another feature that limits the usage of conventional polyurethane materials is lack of, or inadequate, transparency. This inconvenience is due to the incompatibility between the hard and soft segments, which induces phase segregation and the appearance of crystallites in hard-segment phase and sometimes also in the soft-segment one, decreasing the amorphous nature of the materials. Segment polarity, length, and crystallizability, the tendency to hard segment–soft segment interaction, overall sample composition, and molar mass are among the factors which have an effect on phase segregation in polyurethanes [2]. It is known that higher polarity polyester and polycarbonate soft segments making up stronger hydrogen bonding with the hard segments exhibit a more limited tendency to phase segregation than lower polarity polyether soft segments [9–11]. The use of shorter segments also causes the growth in phase mixing [3, 12–14]. At the same time, a decrease in polymer crystallinity may be achieved by applying mixed or branched chain extenders [15–17] as well as copolymer diols [16, 18]. Transparent, non-yellowing polyurethanes are attractive for use in a variety of applications. They can be applied as interlayers or inner layers in automobile laminated windscreens and

shatterproof coatings for glass containers and so on [16]. In addition, the production of primary and secondary dressings, blood tubing, catheters, cannulae, pacemakers, neurostimulators, and orthopedic nail encapsulation, etc. may include transparent polyurethanes as components [19].

The major aim of the experiment undertaken was to check the possibility of synthesizing highly transparent TPUs containing polyether or polycarbonate soft segment with a relatively low molar mass, i.e., poly(oxytetramethylene) diol (PTMO) of $\overline{M}_n = 1000$ g/mol or poly(hexane-1,6-diyl carbonate) diol (PHCD) of $\overline{M}_n = 860$ g/mol and the hard segment built from HMDI and aliphatic–aromatic sulfur-containing chain extender, i.e., 2,2′-[sulfanediylbis(benzene-1,4-diyloxy)]diethanol (OSOE). Using aliphatic isocyanate and the chain extender with specific structure (no possibility of forming colored benzenoid (quinonoid) structures) makes it possible to synthesize non-yellowing polymers [20]. These segmented polyurethanes (SPURs) in view of the presence of sulfur atoms may show improved adhesive properties to metals [20–26] and higher refractive index [20, 23–26] in comparison with the conventional polyurethanes derived from the butane-1,4-diol (BD) chain extender. To be able to make such a comparison, their analogs based on BD, PTMO or PHCD and HMDI were prepared in the same conditions as SPURs.

Moreover, the work studies the influence of the kind and amount of soft segment on the properties of the synthesized polymers. For all the SPURs, physicochemical, optical, thermal, and mechanical properties were determined, and for selected ones, also adhesive properties were determined.

To facilitate the interpretation of the results received, the study also contains data obtained for the regular polyurethane (RPUR), derived from the diol OSOE and HMDI, which is a model of hard segments in these SPURs, as well as polymer diols used as soft segments, although some of them have already been presented [20, 22].

Experimental

Materials

The diol OSOE (m.p. = 101–102 °C after recrystallization first from methanol/water and next from 1,2-dichloroethane) was prepared from 4,4′-sulfanediyldiphenol and ethylene carbonate by a modified procedure described by Penczek et al. [27]. HMDI (99.5%, Desmodur W®) was kindly supplied from Bayer (Germany) and used as received. PHCD of $\overline{M}_n = 860$ g/mol and PTMO of $\overline{M}_n = 1000$ g/mol were purchased from Sigma-Aldrich (USA), and prior to use, they were heated at 90 °C in vacuo for 10 h. Dibutyltin dilaurate (DBTDL) from Merck–Schuchardt (Germany) was used as received, while BD from POCH (Poland) was distilled at 118 °C/18 mm Hg.

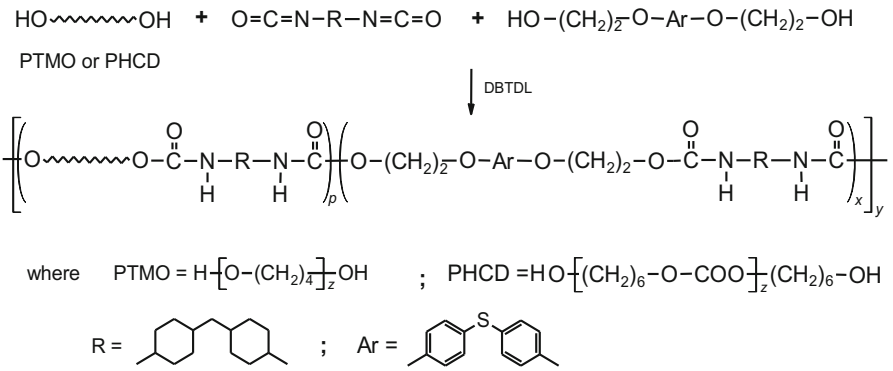

Scheme 1 Synthesis of SPURs

Polymer synthesis

The SPURs, containing 40, 50, or 60 mol% of the soft segment, were obtained in accordance with Scheme 1 by a catalyzed one-step melt polyaddition of the diol OSOE, HMDI, and PTMO or PHCD at the NCO/OH molar ratio of 1.05.

The typical procedure for the synthesis of the SPURs followed the formula: the diol OSOE, PTMO, or PHCD (0.01 mol together) and HMDI (0.0105 mol) were heated with stirring under dry nitrogen to 110 °C in an oil bath. A catalytic amount of DBTDL (about 3.2×10^{-5} mol) was added to the formed clear melt and polymerization rapidly began at vigorous stirring. The mixing was continued until the viscosity increase made stirring impossible. The reaction temperature was gradually raised to 135 °C and the formed product was additionally heated at this temperature for 2 h.

Measurement methods

Reduced viscosities (η_{red}s, dL/g) of 0.5% polymer solution in 1,1,2,2-tetrachloroethane (TChE) were measured in an Ubbelohde viscometer (Poland) at 25 °C.

Number ($\overline{M}_n$) and mass ($\overline{M}_w$) average molar masses, and the molar-mass dispersity (ĐM, $Đ\mathrm{M} = \overline{M}_w/\overline{M}_n$) of the polymers were determined by gel permeation chromatography (GPC) using a Viscotek GPC Max instrument (USA) equipped with Triple Detector Array TDA305. Tetrahydrofuran (THF) was used as an eluent (flow = 1 cm^3/min). The operation temperature was set at 35 °C and a sample concentration of 5 mg/cm^3 was applied. The molar mass was calibrated with polystyrene standards.

Elemental analysis was performed with a Perkin–Elmer CHN 2400 analyzer (USA).

The Fourier transform infrared (FTIR) spectra were recorded with a Bruker Tensor 27 FTIR spectrometer (Germany) using the attenuated total reflectance (ATR) technique. All spectra were obtained at room temperature after averaging 32 scans between 600 and 4000 cm^{-1} with a resolution of 4 cm^{-1} in the absorbance

mode. The infrared carbonyl stretching region of the polymers was resolved into Gaussian curves using OPUS 7.2 software.

The ultraviolet–visible (UV–Vis) spectra were collected with a UV-1800 (Shimadzu, Japan) UV spectrophotometer in the range of 300–900 nm, with a sampling interval of 0.5 nm. The polymers were in the form of the compression-molded 1-mm-thick sheets.

Differential scanning calorimetry (DSC) was carried out using a Netzsch DSC 204 calorimeter (Germany) operating in a dynamic mode. The dynamic scans were performed at the heating/cooling rate of 10 °C/min under nitrogen atmosphere (flow = 30 cm^3/min) from −100 to 200 °C. All DSC measurements were done in aluminum pans with pierced lid (mass of 40 ± 1 mg). As a reference, empty aluminum crucible was applied. Sample masses of 10.0 ± 0.2 mg were used. The reported transitions came from the first and second heating scans. Glass-transition temperatures (T_gs) for the samples were defined as the inflection point on the curves of the heat-capacity changes, and the melting temperatures (T_ms) as endothermic peak maxima.

Thermogravimetry (TG) was performed with a Netzsch STA 449 F1 Jupiter thermal analyzer (Germany) in the range of 40–1000 °C in helium (flow = 20 cm^3/min) and synthetic air (flow = 40 cm^3/min), at the heating rate of 10 °C/min. All TG measurements were taken in Al_2O_3 crucibles (mass of 160 ± 1 mg). As a reference, empty Al_2O_3 crucible was employed. Sample masses of 10.0 ± 0.1 mg were used. The composition of the gas evolved during the decomposition process was analyzed by a Bruker Tensor 27 FTIR spectrometer (Germany) coupled online to a Netzsch STA instrument by Teflon transfer line with 2-mm diameter heated to 200 °C. The FTIR spectra were recorded in the spectral range of 600–4000 cm^{-1} with 16 scans per spectrum at 4-cm^{-1} resolution.

The Shore hardness tests were carried out with a Zwick 7206/H04 durometer (Germany), type A and D. The measurements were taken after 15 s at the temperature of 23°C.

Tensile testing was performed on a Zwick/Roell Z010 (Germany) tensile-testing machine according to Polish Standard PN-81/C-89034 (EN ISO Standard 527–1:1996 and 527–2:1996) at the speed of 100 mm/min at 23 °C; tensile test pieces of 1-mm-thick and 6-mm-wide (for the section measured) were cut from the pressed sheet.

Press moulding was done with a Carver hydraulic press (USA) under 10–30-MPa pressure.

The single lap shear strength of the polymers to copper plate, 100 mm × 25 mm × 1.5 mm, was measured in accordance with Polish Standard PN–EN 1465:2009 using a Zwick/Roell Z010 (Germany). The adhesive joint, 12.5 mm × 25 mm × 0.2 mm, was prepared by pressing the polymer between the ends of two copper plates at 115–120 °C (prepared according to PN–EN-13887:2005), and then leaving them under a pressure of 30 MPa to cool to room temperature. Next, the plates were fixed by tensile-testing machine clips and underwent tensile testing, the speed of 2 mm/min at 23 °C.

Refractive index measurements were done at 23 °C by a Conbest Abbe's Refractometer Type 325 instrument (Poland) in keeping with method A of European

Standard EN ISO 489:1999. 1-Bromonaphthalene was used between the sample film and the prism shield.

Results and discussion

The SPURs were colorless transparent materials (see images for samples PT-50 and PH-50 given in Fig. 1). They did not turn yellow after a long exposure (6 months) to atmospheric conditions at room temperature in contrast to the earlier obtained MDI-derived ones [21, 25]. These materials showed various resistance against common organic solvents. The less resistant were the SPURs based on PHCD, which completely dissolved at room temperature in TChE, *N,N*-dimethylformamide (DMF), *N,N*-dimethylacetamide (DMAc), *N*-methyl-2-pyrrolidone (NMP), and THF. The PTMO-based ones dissolved at room temperature in TChE and THF and at elevated temperature in NMP, but they were partially soluble in DMF and DMAc. Their worse solubility was probably caused by a higher degree of microphase separation. All the SPURs, however, were insoluble in dimethyl sulfoxide.

As can be seen in Table 1, high η_{red} values (2.1–2.9 dL/g) determined for all these polymers suggest their high molar masses. It was verified by GPC measurements. The SPURs exhibited $\overline{M}_n$ included in the range of 50×10^3–81×10^3 g/mol and $\overline{M}_w$ in the range of 88×10^3–165×10^3 g/mol, with higher $\overline{M}_w$ values shown by those based on PHCD. They were also characterized by a relatively low molar-mass dispersity, ranging from 1.26 to 2.96, as for the polymers obtained by melt polymerization method. However, the SPURs derived from PHCD, which were plasticized in slightly higher temperatures, exhibited somewhat higher molar-mass dispersity compared with those from PTMO (see pressing temperature in Table 6). Polymers with similar molar-mass dispersity were also obtained by other authors [18, 28, 29].

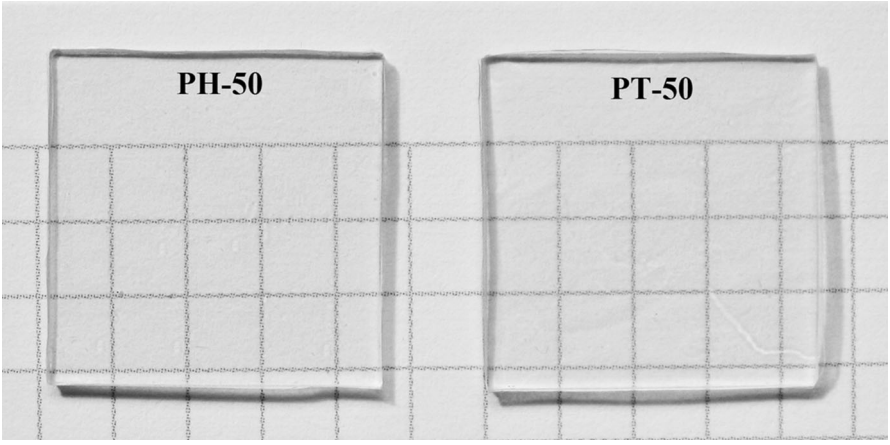

Fig. 1 Images of SPURs PH-50 and PT-50

Table 1 Designations, η_{red}, GPC, transmittance, and refractive index data of the SPURs

SPUR	Soft segment	Soft-segment content (mol%)	Hard-segment content[a] (mas%)	η_{red} (dL/g)	GPC			Transmittance (%)		Refractive index
					$\overline{M}_n$ (g/mol)	$\overline{M}_w$ (g/mol)	ĐM	T^b_{500}	T^b_{800}	
PT-40	PTMO	40	53.4	2.7	68×10^3	104×10^3	1.52	76.9	82.4	1.528
PT-50		50	46.2	2.9	81×10^3	133×10^3	1.64	73.9	77.0	1.520
PT-60		60	39.9	2.1	70×10^3	88×10^3	1.26	71.7	74.9	1.504
PH-40	PHCD	40	57.2	2.2	80×10^3	165×10^3	2.06	87.2	89.0	1.536
PH-50		50	49.9	2.1	73×10^3	159×10^3	2.19	81.6	85.0	1.528
PH-60		60	43.6	2.3	50×10^3	148×10^3	2.96	80.4	84.5	1.523

[a] Hard-segment content $= \frac{\text{HMDI} + \text{OSOE(mass)}}{\text{PTMO/PHCD} + \text{HMDI} + \text{OSOE(mass)}} \times 100\%$..

[b] Transmittance data at 500 and 800 nm

The chemical structures of all the SPURs were examined by elemental analysis and ATR–FTIR spectroscopy.

The results of CHN analysis of all these compounds agreed with the calculated values, as shown below.

PT-40: calcd: C, 65.89%; H, 9.18%; N, 3.42%; found: C, 65.73%; H, 9.39%; N, 3.53%.
PT-50: calcd: C, 65.95%; H, 9.51%; N, 3.17%; found: C, 65.90%; H, 9.65%; N, 3.25%.
PT-60: calcd: C, 66.00%; H, 9.78%; N, 2.95%; found: C, 65.96%; H, 10.02%; N, 3.19%.
PH-40: calcd: C, 64.21%; H, 8.20%; N, 3.66%; found: C, 63.60%; H, 8.21%; N, 3.84%.
PH-50: calcd: C, 62.61%; H, 8.21%; N, 3.42%; found: C, 61.93%; H, 8.33%; N, 3.42%.
PH-60: calcd: C, 62.23%; H, 8.35%; N, 3.22%; found: C, 61.52%; H, 8.46%; N, 3.25%.

ATR-FTIR spectra were consistent with the proposed structures of the SPURs. No isocyanate peak about 2270 cm^{-1} was seen in any spectra, indicating full NCO conversion. The main absorption bands are given below, whereas representative spectra are shown in Fig. 2. In addition, the deconvolution of the carbonyl stretching region for all the SPURs and PHCD was done and the obtained results are given in Tables 2 and 3, and Figs. 2 and 3.

SPURs from PTMO (cm^{-1}): 1526–1525 (N–H bending), 3327–3325 (N–H stretching), and 1717–1716 and 1702–1699 (non-H–bonded and H–bonded C=O stretching) of the urethane group; 1226 (coupled C–N and C–O stretching of the urethane group and asymmetric C–O–C stretching in aliphatic–aromatic ether); 1100 (asymmetric C–O–C stretching) in aliphatic ether; 2928–2924 and 2852 (asymmetric and symmetric C–H stretching) and 1449–1448 (asymmetric C–H bending) of CH_2; 1594–1593 and 1491 (C–C stretching) of benzene ring; and 825–824 (C–H bending) of *p*-disubstituted benzene ring.

SPURs from PHCD (cm^{-1}): 1522 (N–H bending) and 3368–3334 (N–H stretching) of the urethane group; 1740–1702 (C = O stretching of the urethane and carbonate groups); 1244–1242 (C–O stretching) of the carbonate group; 1218 (coupled C–N and C–O stretching of the urethane group and asymmetric C–O–C stretching in aliphatic–aromatic ether); 1048–1044 (symmetric C–O–C stretching in aliphatic–aromatic ether); 791 (out-of-plane bending of O–CO–O); 2927–2925 and 2856–2855 (asymmetric and symmetric C–H stretching) and 1454 (asymmetric C–H bending) of CH_2; 1593 and 1492 (C–C stretching) of benzene ring; and 826–825 (C–H bending) of *p*-disubstituted benzene ring.

For the PTMO-based SPURs, the carbonyl stretching region can be split into three contributions: band I at 1720 cm^{-1}, band II at 1698–1697 cm^{-1}, and band III at 1664–1659 cm^{-1}. Band I can be attributed to the non-H-bonded urethane carbonyl groups, while band II can be assigned to H-bonded ones in amorphous hard-segment domains [23]. In the case of the PHCD-based SPURs, carbonyl

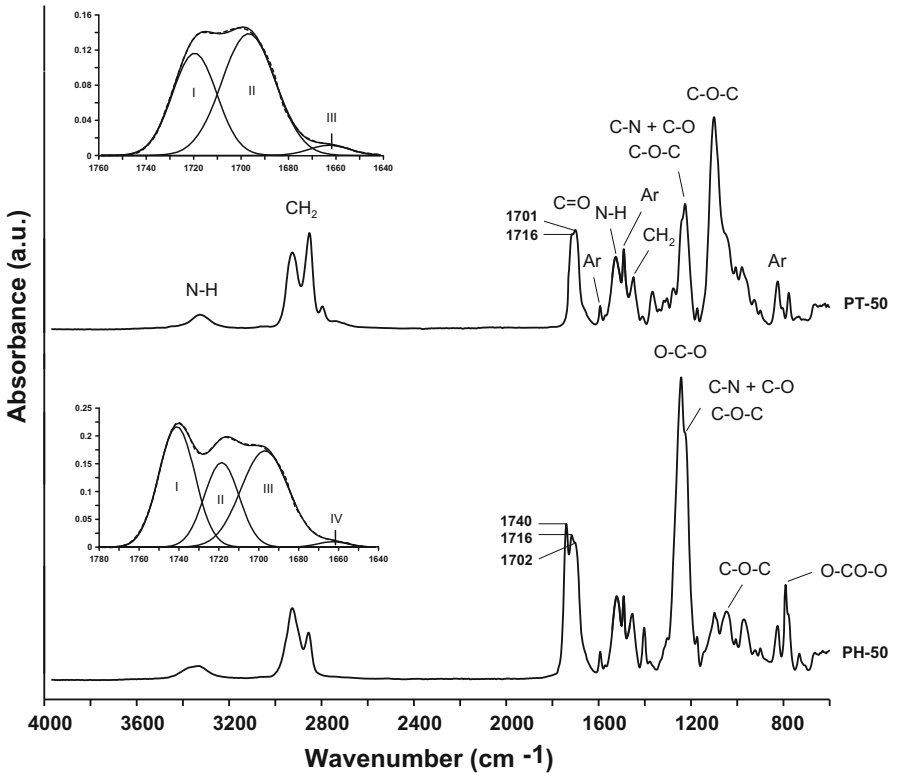

Fig. 2 FTIR spectra and the deconvolution of the carbonyl stretching region of SPURs PT-50 and PH-50 (*dashed line* recorded spectra; *solid line* resolved peaks)

Table 2 Characteristics of the carbonyl stretching region of the SPURs based on PTMO

SPUR	Band I		Band II		Band III	
	υ (cm^{-1})	Area (%)	υ (cm^{-1})	Area (%)	υ (cm^{-1})	Area (%)
PT-40	1720	33.9	1697	61.5	1659	4.6
PT-50	1720	39.4	1697	57.0	1663	3.6
PT-60	1720	41.0	1698	56.8	1664	2.2

stretching region was composed of four bands: I at 1742–1741 cm^{-1}, II at 1719–1718 cm^{-1}, III at 1698–1695 cm^{-1}, and IV at 1664–1663 cm^{-1}. Considering the deconvolution of PHCD (see Fig. 3) and SPURs derived from PTMO, band I should correspond to the non-H-bonded carbonate carbonyl groups, and band II to the H-bonded carbonate carbonyl groups and the non-H-bonded urethane carbonyl groups, whereas band III to the H-bonded urethane ones. It is not possible to clearly ascribe the band occurring in both series at the lowest wavenumber, whose share is

Table 3 Characteristics of the carbonyl stretching region of the SPURs based on PHCD

SPUR	Band I		Band II		Band III		Band IV	
	υ (cm^{-1})	Area (%)	υ (cm^{-1})	Area (%)	υ (cm^{-1})	Area (%)	υ (cm^{-1})	Area (%)
PH-40	1742	29.1	1718	31.2	1695	37.6	1664	2.1
PH-50	1741	36.0	1719	24.4	1697	38.2	1663	1.4
PH-60	1741	39.6	1719	21.1	1698	37.9	1663	1.4

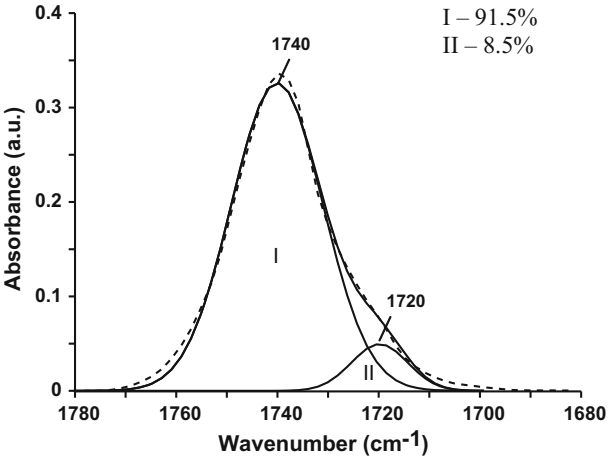

Fig. 3 Deconvolution of the carbonyl stretching region of PHCD (*dashed line* recorded spectra; *solid line*: resolved peaks)

low (1.4–4.6%), to the structure of these amorphous polymers. In general, this absorption region corresponds to the H-bonded urethane carbonyl groups in crystalline hard-segment domains [30].

In PTMO series, samples PT-50 and PT-60 are characterized by smaller shares of H-bonded urethane carbonyl groups and higher fractions of the non-H-bonded ones in comparison with sample PT-40. Moreover, in the case of the former samples, no influence of composition on these shares is observed. These polymers showed similar and much higher degree of microphase separation than polymer PT-40 (see DSC data from the second heating scans).

As regards the PHCD series, fractions of the H-bonded urethane carbonyl groups were practically the same. Thus, the extent of interurethane interaction did not depend on the content of the soft segments. On the other hand, an increase of the soft-segment content was accompanied by an increase in the fraction of the non-H-bonded carbonate carbonyl groups, indicating a drop in the extent of urethane–carbonate interaction. The consequence is a growth of the degree of microphase separation.

Thermal properties

TG

A TG analysis was conducted in inert atmosphere (helium) for all the synthesized SPURs and in oxidative atmosphere (air) for selected ones, i.e. PT-50 and PH-50. Table 2 compiles characteristic temperatures for the degradation process of the SPURs, i.e., T_1, T_5, T_{10}, T_{50}, and T_{max}, that refer to the temperatures of 1, 5, 10, and 50% mass loss and of the maximum rate of mass loss. Table 4 also gives the temperatures received for the RPUR, PTMO, and PHCD, while those obtained in inert atmosphere have already been demonstrated [20, 22].

As is evident from the data contained in Table 4, in helium, the SPURs from PTMO revealed higher T_1, T_5, T_{10}, and T_{50} than analogous ones from PHCD, due to the worse thermal stability of the polycarbonate soft segments than that of the polyether soft segments. In both series, they were almost independent of soft-segment content.

From the course of DTG curves, it results that in helium, the SPURs of both types decomposed in two stages. The curves of the SPURs with a PTMO soft segment (see Fig. 4) depicted two overlapping large intense peaks with maxima at 347–353 °C and 406 °C. With the increase of the soft-segment content, an increase of the peak intensity at 406 °C and a decrease at ~350 °C were observed. The curves of the SPURs with a PHCD soft segment (see Fig. 5) also displayed two overlapping peaks, with maxima at 333–337 and 398–404 °C, with a much higher intensity revealed by the first one. Herein, dissimilarly, the increase of the soft-segment content caused an increase of the peak intensity at lower temperature, and a decrease at higher temperature. On the basis of the analysis of the DTG data of these SPURs and those of the RPUR and polymer diols, it may be stated that the

Table 4 TG data of the polymers

Polymer	T_1^a (°C)		T_5^b (°C)		T_{10}^c (°C)		T_{50}^d (°C)		T_{max}^e (°C)	
	Helium	Air	Helium	Air	Helium	Air	Helium	Air	Helium	Air
RPUR	275	276	300	309	318	323	353	358	360, 449	354, 390, 515
PT-40	270		301		316		363		347, 406	
PT-50	274	255	305	294	320	313	372	360	353, 406	352, 407, 521
PT-60	274		303		318		375		349, 406	
PTMO	269	177	326	194	347	204	402	238	415	252
PH-40	259		282		296		338		336, 398	
PH-50	258	267	281	300	295	312	337	347	337, 400	343 405, 528
PH-60	258		281		294		334		333, 404	
PHCD	209	168	264	218	290	241	352	313	364	333, 470

[a, b, c, d] The temperature of 1, 5, 10, and 50% mass loss from the TG curve, respectively

[e] The temperature of the maximum rate of mass loss from the DTG curve

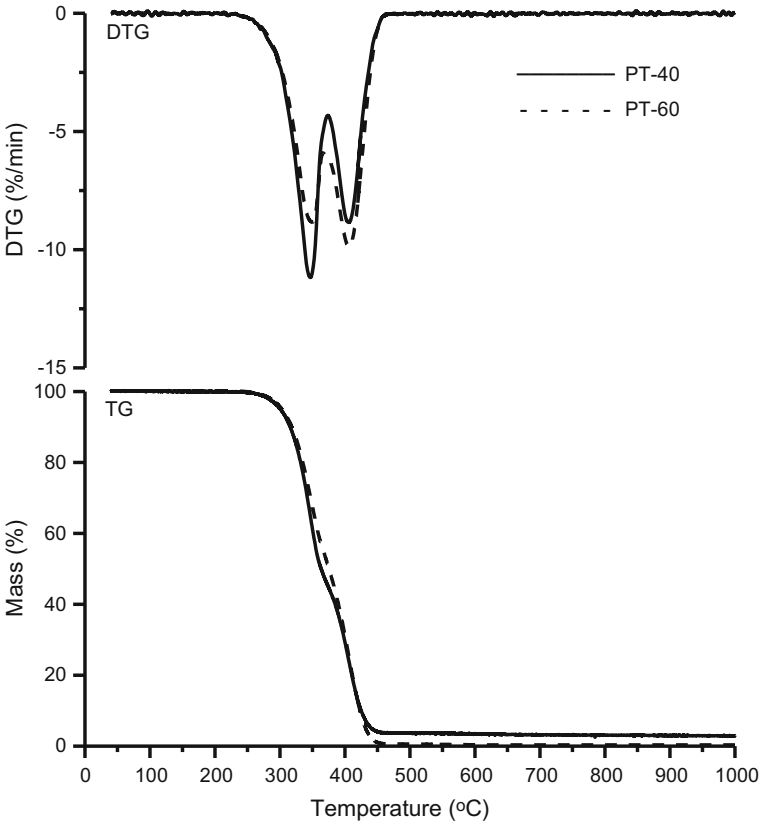

Fig. 4 DTG and TG curves of the SPURs based on PTMO in helium

decomposition of the SPURs based on PTMO started from the hard segments, partly superimposed on which was the decomposition of soft segments; in the case of the SPURs based on PHCD, the main decomposition of the hard segments took place together with the decomposition of the soft segments.

When comparing the data received for SPURs PT-50 and PH-50 in helium and air (Table 4), it is clear that thermal stability of these SPURs variably depended on the testing atmosphere. PT–50 containing polyether soft segments resistant to oxidation to a low degree [31] revealed poorer stability (lower T_1, T_5, T_{10}, and T_{50}) in air. Considering PH-50 with polycarbonate soft segments resistant to oxidation, enhanced stability was observed on the contrary. It ought to be explained by the oxidation processes that stabilize hard segments with diphenyl sulfide units [32]. In oxidative atmosphere, both these SPURs and RPUR, decomposed in three stages (see Fig. 6). On DTG curves, there appeared an additional peak of low intensity with maximum at 515–528 °C, connected with the oxidation of nonvolatile residue obtained in the previous stages.

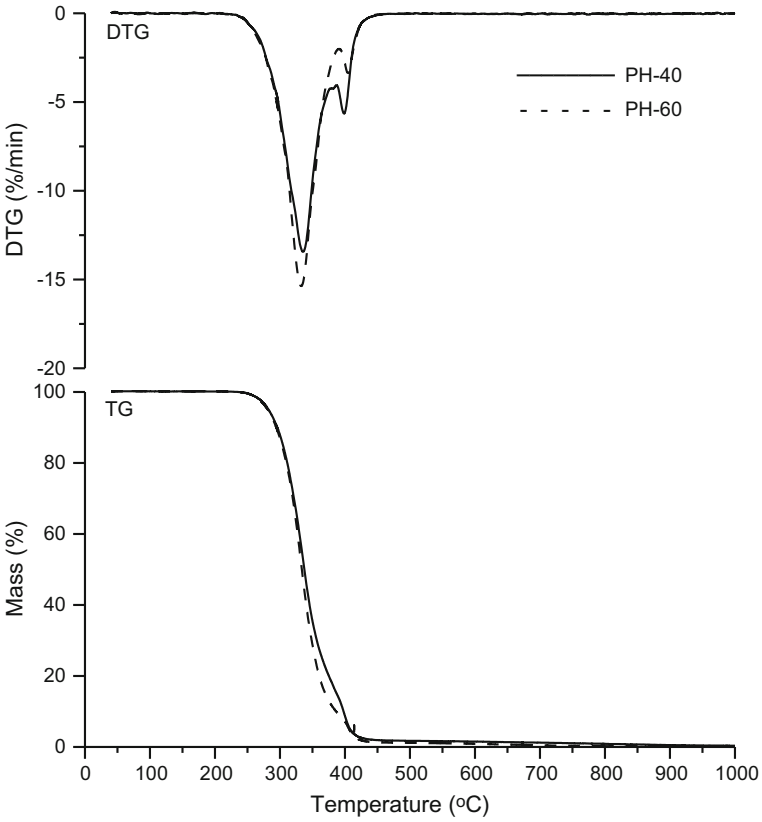

Fig. 5 DTG and TG curves of SPURs based on PHCD in helium

TG-FTIR

To gain a deeper look into the decomposition process of the polymers, the TG coupled with FTIR spectroscopy (TG-FTIR) was applied. The analysis was performed for polymers PT-50, PH-50, PTMO, and PHCD, both in inert and oxidative atmosphere, and for RPUR only in oxidative atmosphere, because the TG-FTIR data received in inert atmosphere were described in the previous paper [20].

The FTIR spectra recorded during the first decomposition stage of SPUR PT-50 in helium (T_{max} at 353 °C) presented in Fig. 7 showed bands typical of carbon dioxide (at 2359–2310 cm^{-1}, attributed to asymmetric stretching vibration and at 669 cm^{-1} attributed to the degenerate bending vibration), carbon monoxide (at ~2186 and 2114 cm^{-1} related to stretching vibration), and water (at ~4000–3500 cm^{-1} associated with stretching vibration and ~1800–1300 cm^{-1} associated with bending vibration). Moreover, the spectra exhibited bands pointing to the presence of aliphatic aldehydes and ethers (at 2964 and 2882 cm^{-1}, characteristic of asymmetric and symmetric C–H stretching vibration of methylene and methyl groups, at 2821 and 2720 cm^{-1}, connected with C–H stretching

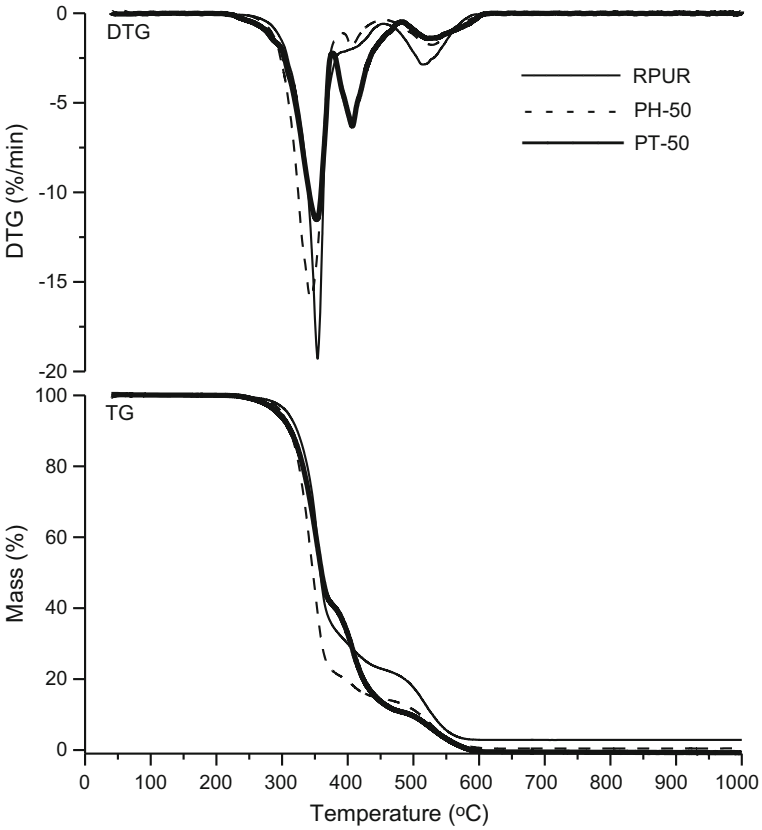

Fig. 6 DTG and TG curves of RPUR and SPURs PT-50 and PH-50 in air

vibration of aldehyde group, and at 1165–1074 cm^{-1}, associated with C–O stretching vibration of ether group) as well as unsaturated compounds (at 950 and 916 cm^{-1}, related to C–H out-of-plane deformation vibration of vinyl group). In the second stage (T_{max} at 406 °C), the same bands as in the first stage were observed, but bands coming from carbon dioxide and water were more intensive.

Similar to the case of SPUR PT-50, the FTIR spectra from the first and second decomposition stages of SPUR PH-50 in helium (Fig. 8) also pointed to the existence of carbon dioxide, carbon monoxide, and water as well as aliphatic aldehydes, ethers, and unsaturated compounds. In the second stage, besides bands at 1136–1060 cm^{-1} characteristic for aliphatic ethers, in addition, a band at 1176 cm^{-1} appeared, which originated from aliphatic–aromatic ethers. The band at 1060 cm^{-1} can also indicate the presence of alcohols (C–O stretching vibration).

Taking into account the spectra obtained from decomposition of RPUR [20] and polymer diols (Figs. 7, 8) in helium, it can be said that aliphatic ethers and aldehydes were connected with the decomposition of soft segments only, whereas aliphatic–aromatic ethers were connected with the decomposition of hard segments only. In addition, water mainly came from the hard-segment decomposition. In all

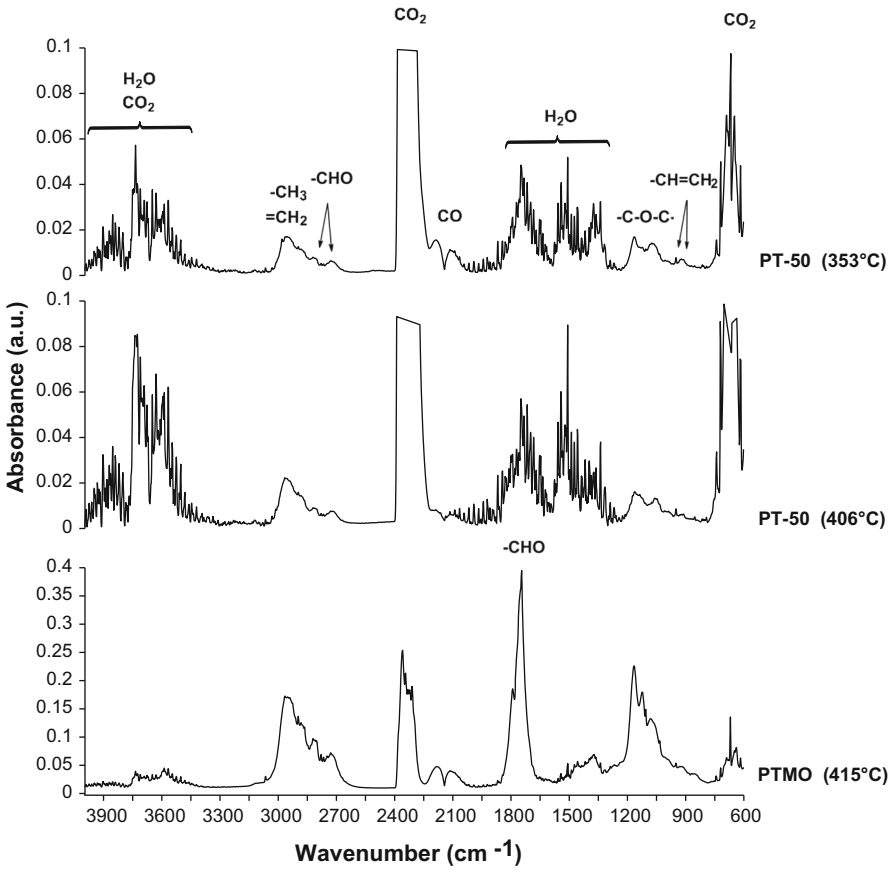

Fig. 7 FTIR spectra of volatile products obtained at the maximum rate of mass loss of the thermal decomposition of polymers PT-50 and PTMO in helium

the SPUR spectra, no bands typical of carbonyl sulfide, being witness of the decomposition of diaryl-sulfide linkages, were detected, which may be caused by the lower share of the hard segments in the structure of these polymers. On the other hand, an intensive evolution of carbon dioxide manifested the decomposition of urethane linkages, and in the case of the PHCD-based SPURs also of carbonate ones. Owing to the fact that amine compounds were not identified at any stage, it may be supposed that decomposition of the urethane linkages was attached to their dissociation to alcohols and isocyanates, followed by the carbodiimization of isocyanates and accompanied by the evolution of carbon dioxide [33, 34].

In the FTIR spectra of the volatile products of RPUR decomposition in air (see Fig. 9) from the first stage (T_{max} at 354 °C), just as in the case of its decomposition in helium [20], one could see absorption bands typical of carbon dioxide, water, unsaturated compounds, and carbonyl sulfide (at 2073 and 2043 cm^{-1}, characteristic of asymmetric and symmetric C=O stretching vibration). There also appeared bands indicating existence of aromatic compounds (at 3048 and 1602 cm^{-1},

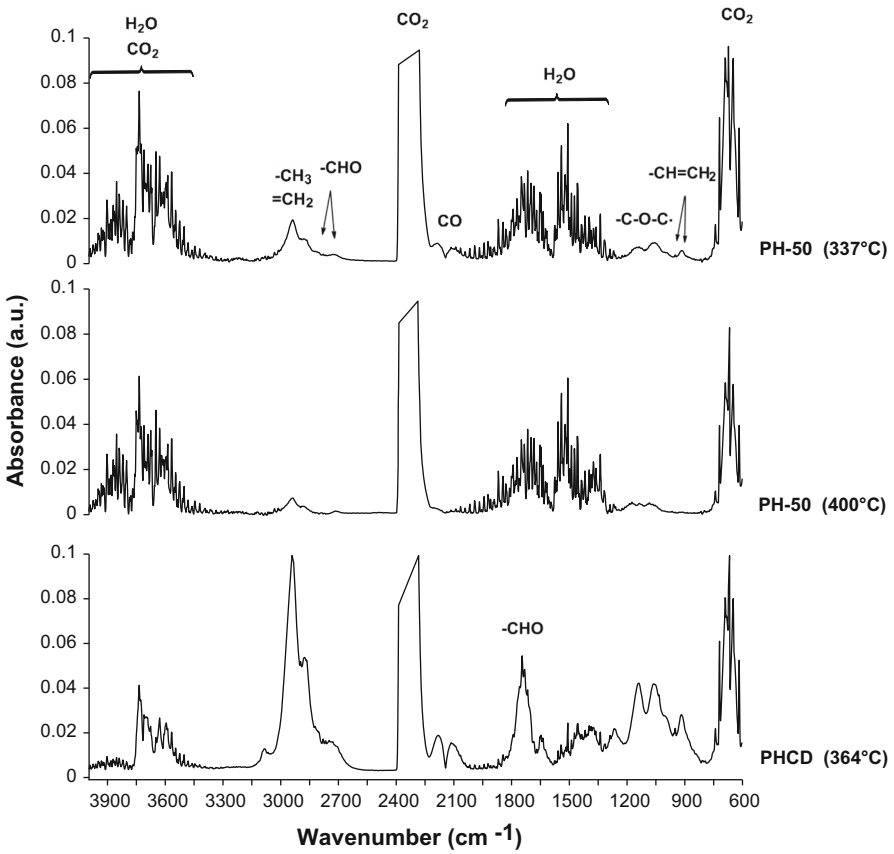

Fig. 8 FTIR spectra of volatile products obtained at the maximum rate of mass loss of the thermal decomposition of polymers PH-50 and PHCD in helium

connected with C–H and C–C stretching vibration of the benzene ring and at 827 cm^{-1}, characteristic of C–H out-of-plane deformation vibration of *p*-disubstituted benzenes), aliphatic–aromatic ethers (at 1244 and 1176 cm^{-1}, associated with C–O stretching vibration of the ether group), and carbon monoxide, which, when decomposition in helium took place, were observable only in the second stage. Moreover, the spectrum displayed bands at 1375–1339 cm^{-1}, which could be attributed to asymmetric stretching vibration in sulfur dioxide. The spectra from the second and third stages (T_{max} at 390 and 515 °C) pointed to the presence of carbon dioxide, carbon monoxide, water, aromatic compounds, and aliphatic–aromatic ethers, but in lesser amounts in comparison with the first stage. It could be noticed that the bands coming from carbon dioxide showed greater intensity in the third stage, in which the oxidation processes were more thorough.

The decomposition of SPURs PT-50 and PH-50 in air was connected as a rule with the elimination of the same products as in inert atmosphere. Figure 10 presents the spectra obtained for polymer PT-50 as an illustration.

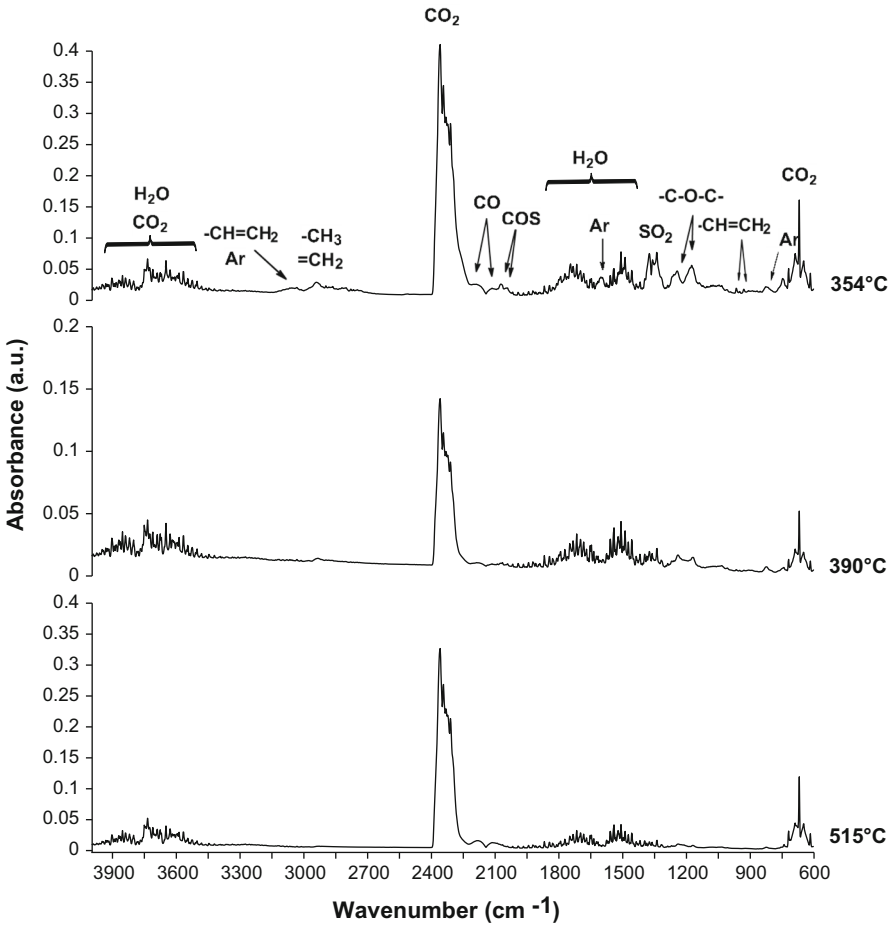

Fig. 9 FTIR spectra of volatile products obtained at the maximum rate of mass loss of the thermal decomposition of RPUR in air

DSC

A DSC analysis was performed in inert atmosphere. Table 5 gives the numerical data (T_g, $T_{m,}$ and heat of melting (ΔH) values) obtained for all the SPURs, while the DSC curves for those with soft-segment content of 40 and 60 mol% are given in Fig. 11. Table 5 and Fig. 11 also contain data received for RPUR as well as PTMO and PHCD.

From the data shown in Table 3, it follows that the SPURs derived from PTMO revealed lower definite T_gs than their analogs derived from PHCD (−29 to 14 °C vs. 11–43 °C). The former polymers exhibited also a higher degree of microphase separation (higher differences between the T_g values of the pure soft segments and the suitable SPURs). The higher degree of separation is the result of a weaker interaction of hard-segment urethane groups with ether oxygen than with carbonate

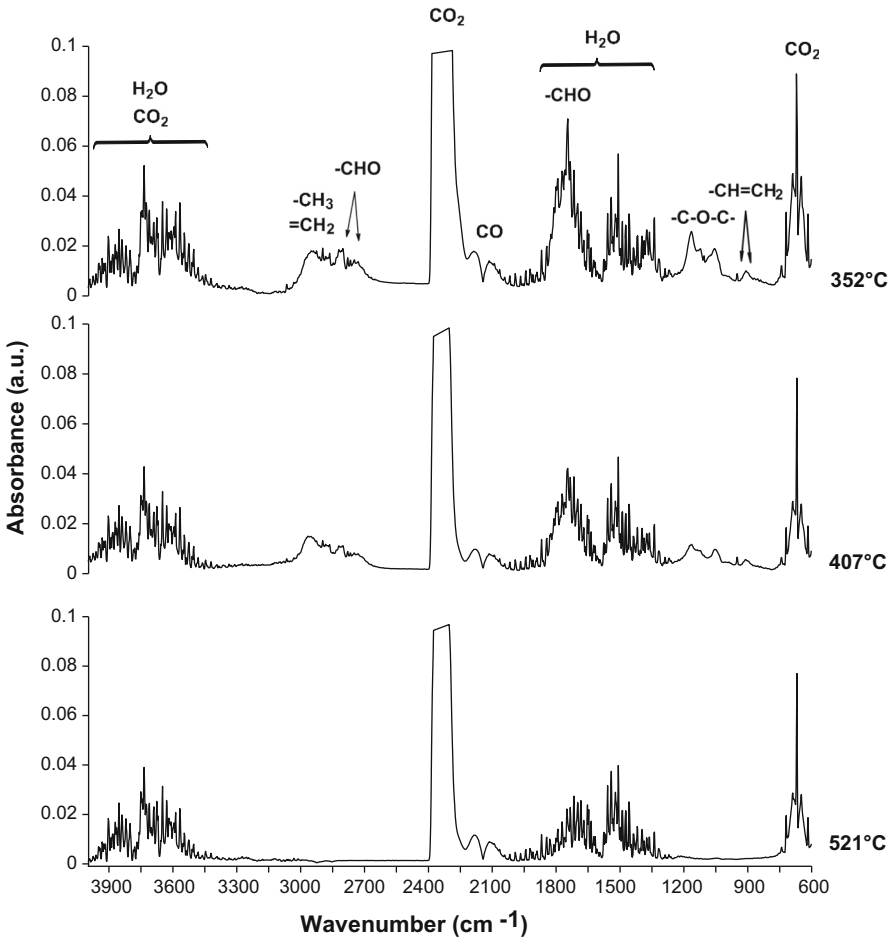

Fig. 10 FTIR spectra of volatile products obtained at the maximum rate of mass loss of the thermal decomposition of SPUR PT-50 in air

carbonyl groups of soft-segment chains. To some degree, the negligible difference in molar masses of soft segments may also influence the phenomenon mentioned above. In both series of the polymers, the increase in soft-segment content caused a decrease in T_g, indicating an increase of the degree of microphase separation. The synthesized SPURs, with the exception of PH-40 and PH-50, showed T_gs below room temperature, characteristic of elastomers.

The DSC curves from the first heating scans of the SPURs containing 40 and 50 mol% PHCD (PH-40 and PH-50) besides glass transition displayed a very small endothermic peak connected with the melting of hard-segment domains at 157 and 186 °C, respectively. On the other hand, the curves obtained for the PH-60 as well as all PTMO-based ones showed only glass transition. The very low heat of melting (ΔH) values ($\sim$1 J/g) observed for polymers PH-40 and PH-50 and lack of the

Table 5 DSC data of the polymers

Polymer	T_g (°C)		T_m (°C)		ΔH (J/g)	
	I[a]	II[a]	I[a]	II[a]	I[a]	II[a]
RPUR	72	94	133, 167		8.7	
PT-40	5	14				
PT-50	–14	–20				
PT-60	–29	–24				
PTMO	–77	–78	16, 30	0, 23	119.6	107.9
PH-40	43	35	157		1.0	
PH-50	31	28	186		1.2	
PH-60	11	14				
PHCD	–69	–63	10, 30	31	55.5	37.2

[a] I and II, first and second heating scans, respectively

endothermic peaks on curves of the remaining SPURs point to their amorphous structures. The DSC curves from the second heating scans exhibited no endothermic peaks for all the investigated SPURs.

Mechanical properties

As results from the data presented in Table 6, the PHCD-based SPURs showed much higher tensile strength (39.8–48.6 MPa vs. 6.8–28.3 MPa) and lower elongation at break (225–300% vs. 400–700%) than the analogous PTMO-based ones. These differences deepen with an increase in the soft-segment content of the polymer. This can be explained by stronger intermolecular interactions in polycarbonate soft segments in comparison with those in polyether ones. Higher tensile strength of the SPURs containing polycarbonate soft segments can also be caused by their higher $\overline{M}_w$. These polymers exhibited higher hardness (79–96°Sh A vs. 59–73°Sh A) and modulus of elasticity (5.5–89.7 MPa vs. 1.4–5.1 MPa) as well. Particularly, high values were shown by PH-40 and PH-50 with T_gs above 30 °C. Their stress–strain curves exhibited yield stress, characteristic of plastomers. The remaining polymers, both of the PTMO and PHCD series, with T_gs in the range of −29 to 11 °C, displayed stress–strain curves, typical of elastomers. Figure 12 shows the stress–strain curves for polymers PT-40, PT-60, PH-40, and PH-60.

In both series, as the soft-segment content increased hardness and the modulus of elasticity decreased, whereas elongation at break increased.

All the obtained SPURs showed significantly higher tensile strength and hardness, but smaller elongation at break than the suitable ones synthesized from diphenylmethane-derivative diol as a chain extender [26].

Optical properties

Table 1 presents the refractive index and transmittance data at 500 and 800 nm obtained for the all synthesized SPURs, whereas the UV–Vis spectra of the selected ones are given in Fig. 13.

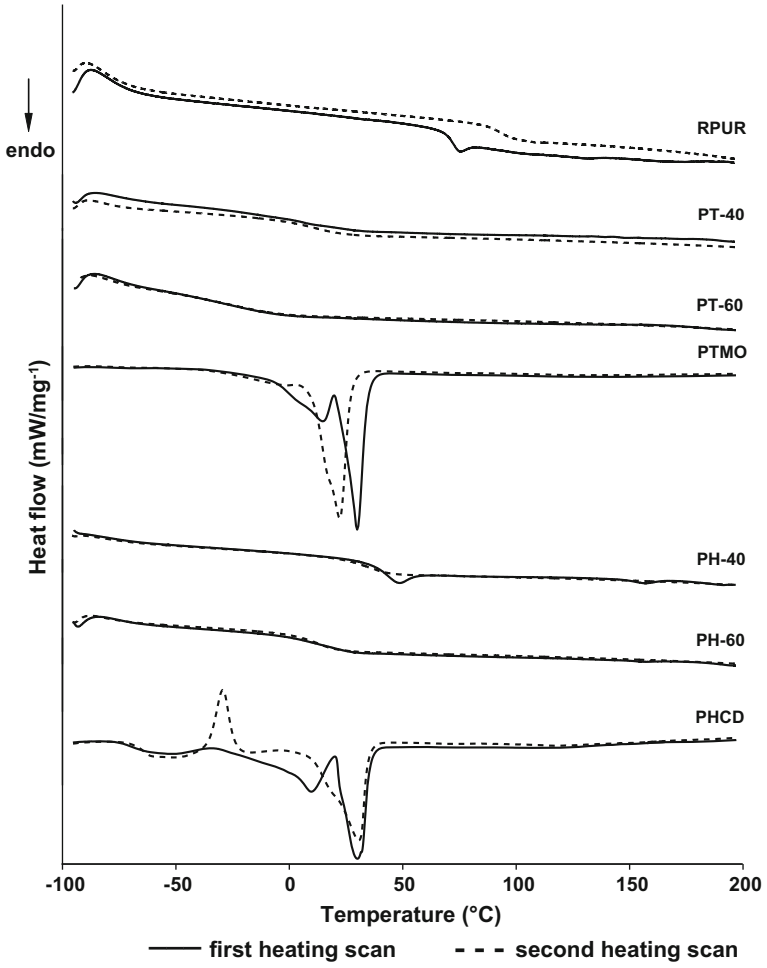

Fig. 11 DSC curves of selected SPURs as well as RPUR, PTMO, and PHCD

From these data it follows that, in both series, an increase of the hard-segment content (i.e., rise in sulfur atoms) resulted in increasing of refractive index of the SPUR. Moreover, higher values were exhibited by the polymers derived from PHCD (1.523–1.536 vs. 1.504–1.528). It is hard to clearly decide whether those differences result from the kind of the soft segment used, or the higher mass content of the hard segments at the same molar content of these segments (see Table 1). Taking into account the results received for poly(thiourethane-urethane)s obtained from the same diisocyanate and soft segments, it is possible to think that the former factor was decisive (the presence of carbonate linkages) [24]. If one compares the SPURs PT-50 and PH-50 and their analogs based on BD chain extender with the same content of the hard segments, it should be stated that the former polymers showed higher values of this parameter (1.520 vs. 1.496 and 1.528 vs. 1.501).

Table 6 Mechanical properties of the SPURs

SPUR	Hardness (°Sh)		Modulus of elasticity (MPa)	Tensile strength (MPa)	Elongation at break (%)	Pressing temperature (°C)
	A	D				
PT-40	73	27	5.1 ± 0.33	28.3 ± 0.63	400 ± 22	120
PT-50	62	22	3.7 ± 0.22	15.0 ± 0.15	600 ± 33	115
PT-60	59	17	1.4 ± 0.03	6.8 ± 0.18	700 ± 40	110
PH-40	96	65	89.7 ± 0.88	47.1 ± 0.74	225 ± 10	140
PH-50	94	49	55.4 ± 0.94	48.6 ± 0.82	250 ± 14	120
PH-60	79	30	5.5 ± 0.06	39.8 ± 0.55	300 ± 25	115

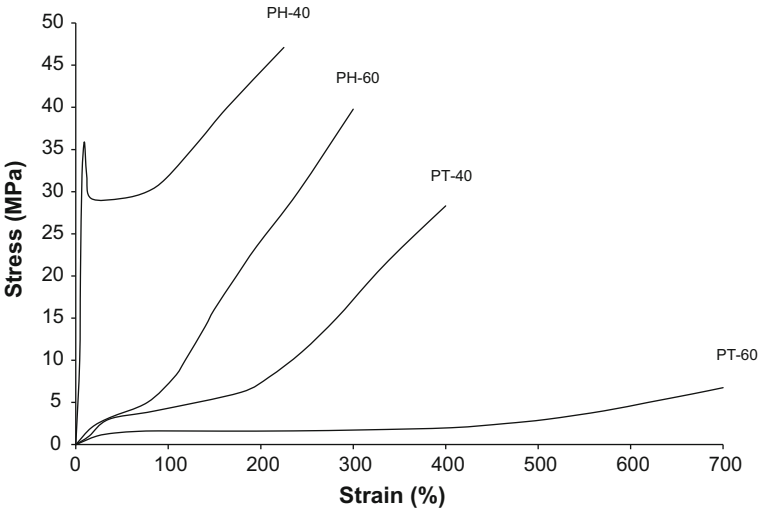

Fig. 12 Stress–strain curves of selected SPURs

The synthesized PHCD-based SPURs also revealed better transparency in comparison with PTMO-based ones and the same dependence was present for the analogs of SPURs PT-50 and PH-50 obtained from BD (transmittance at 500 and 800 nm: 75.9 and 82.1% (with PHCD soft segments) and 65.6 and 71.9% (with PTMO soft segments). This is caused by better miscibility of the polycarbonate soft segments and hard segments than the polyether soft segments and hard segments (see T_g values in Table 2). In both series, transparency changed in the same direction as refractive index. The same dependence was seen for the above-mentioned poly(thiourethane-urethane)s [24].

From the analysis carried out, it results that the deciding impact on transparency was had by the phase mixing of soft and hard segments, whereas the refractive index values depended on the content of sulfur atoms.

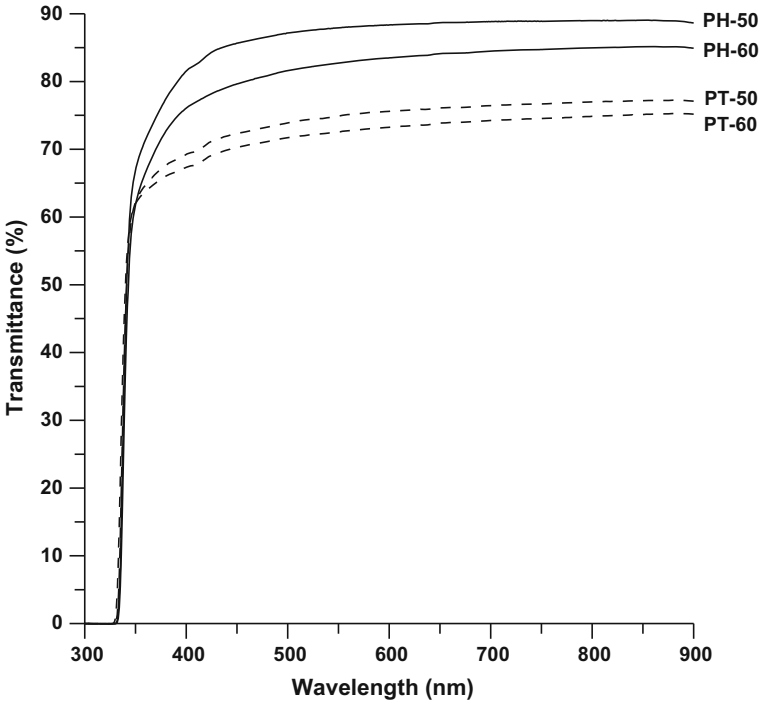

Fig. 13 UV–Vis spectra of selected SPURs

Adhesive properties

The influence of sulfur-containing chain extender on the lap shear strengths to copper (adhesion) of the obtained SPURs was investigated for polymers with 50 mol% soft-segment content, i.e., PT-50 and PH-50 and their BD-derived analogs. The obtained results are presented in Fig. 14. They reveal that both polymers PT-50 and PH-50 showed over eight times higher adhesive strength than those from BD (4.2 and 9.2 MPa vs. 0.5 and 1.1 MPa).

Adhesion to polar materials, such as glass, metal, or wood, largely depends on the number of polar groups and the size of the dipole moment [3]. Hence, higher lap shear strengths to copper were found for polymers based on diol OSOE (more polar groups), as well as those based on PHCD (a higher dipole moment of carbonate group than that of ether group).

Conclusions

New thermoplastic polyether- and polycarbonate-based SPURs were synthesized by a catalyzed one-step melt polyaddition from 2,2′-[sulfanediylbis(benzene-1,4-diyloxy)]diethanol as a nonconventional chain extender, HMDI, and 40, 50, and 60 mol% PHCD of $\overline{M}_n$ = 860 g/mol, or PTMO of $\overline{M}_n$ = 1000 g/mol as soft

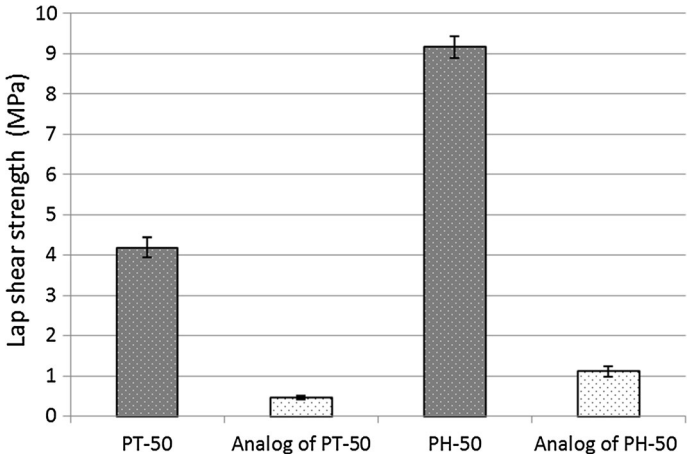

Fig. 14 Lap shear strength of SPURs PT-50 and PH-50 and their analogs based on BD

segments. The obtained colorless, transparent, high molar-mass materials exhibited amorphous structures. A better transparency (transmittance at 800 nm: 84–89% vs. 75–82%) was shown by the polymers with the PHCD soft segments. As it follows from DSC analysis, all the SPURs of PTMO series and one of PHCD series (PH-60) turned to be TPUs. Lower T_gs (from −29 to 14 °C vs. from 11 to 43 °C) and better microphase separation were exhibited by the former polymers. A TG study revealed that all the SPURs possessed a relatively good thermal stability, though dependent on both the kind of soft segment and the testing atmosphere. Their temperatures of 1% mass loss were contained within the range of 255–274 °C. In helium, higher values were shown by those from PTMO, while in air, the situation was reversed. The polymers decomposed in two (in helium) or three (in air) stages. The testing atmosphere, however, did not significantly influence the type of volatile products emitted. In both cases, the degradation process was connected with the elimination of carbon dioxide, carbon monoxide, water, aliphatic–aromatic ethers, aliphatic aldehydes, and ethers as well as unsaturated compounds. Results obtained from the analysis of mechanical properties demonstrated that the SPURs derived from PHCD showed much higher tensile strength (39.8–47.1 MPa vs. 6.8–28.3 MPa) and elongation at break (225–300% vs. 400–700%) than those synthesized from PTMO. Moreover, the PHCD-based TPU PH-60, with hardness of 79°Sh A, possessed better tensile strength (39.8 MPa) and smaller elongation at break (300%) than the commercial biodurable medical grade TPU with an HMDI/BD hard segment and poly(hexane-1,6-diyl-ethylene carbonate) diol soft segment, i.e., ChronoFlex® AL 80A (37.9 MPa, 585%) [35]. Among the PTMO-based TPUs, PT–40 showed higher tensile strength (28.3 MPa) at smaller elongation at break (400%) in comparison with the commercial polyether-based aliphatic TPU Lubrizol Estane® AG 4350 (24.1 MPa, 550%) [35]. The newly synthesized sulfur-containing polymers showed better transparency, higher refractive index, and adhesive strength to copper than analogous polymers based on BD as a chain extender.

References

1. Ulrich H (2003) Polyurethanes. In: Mark HF (ed) Encyclopedia of polymers science and technology, vol 4. Wiley, New Jersey, pp 26–72
2. Gogolewski S (1989) Selected topics in biomedical polyurethanes. A review. Colloid Polym Sci 267:757–785
3. Wirpsza Z (1993) Polyurethanes: chemistry, technology and applications. Ellis Horwood, New York
4. Wilhelm C, Rivaton A, Gardette JL (1998) Infrared analysis of the photochemical behaviour of segmented polyurethanes – 3. Aromatic diisocyanate based polymers. Polymer 39:1223–1232
5. Boubakri A, Guermazi N, Elleuch K, Ayedi HF. Study of UV-aging of thermoplastic polyurethane material. Mater Sci Eng A 527:1649–1654
6. Rosu D, Rosu L, Cascaval CN (2009) IR-change and yellowing of polyurethane as a result of UV irradiation. Polym Degrad Stabil 94:591–596
7. Tcharkhtchi A, Farzaneh S, Abdallah-Elhirtsi S, Esmaeillou B, Nony F, Baron A (2014) Thermal aging effect on mechanical properties of polyurethane. Int J Polym Anal Char 19:571–584
8. Wilhelm C, Gardette JL (1997) Infrared analysis of the photochemical behaviour of segmented polyurethanes: 1. Aliphatic poly(ester-urethane). Polymer 38:4019–4031
9. Bagdi K, Molnar K, Sajo I, Pukanszky B (2011) Specific interactions, structure and properties in segmented polyurethane elastomers. Express Polym Lett 5:417–427
10. Kultys A, Rogulska M, Gluchowska H (2011) The effect of soft-segment structure on the properties of novel thermoplastic polyurethane elastomers based on an unconventional chain extender. Polym Int 60:652–659
11. Kultys A, Rogulska M, Pikus S (2012) New thermoplastic segmented polyurethanes with hard segments derived from 4,4′-diphenylmethane diisocyanate and methylenebis(1,4-phenylenemethylenethio)dialcanols. J Appl Polym Sci 123:331–346
12. Kim BK, Shin YJ, Cho SM, Jeong HM (2000) Shape-memory behavior of segmented polyurethanes with an amorphous reversible phase: the effect of block length and content. J Polym Sci B Polym Phys 38:2652–2657
13. Martin DJ, Meijs GF, Renwick GM, McCarthy SJ, Gunatillake PA (1996) The effect of average soft segment length on morphology and properties of a series of polyurethane elastomers. 1. Characterization of the series. J Appl Polym Sci 62:1377–1386
14. Gomez CA, Gutierez D, Asensio M, Costa V, Nohales A Transparent thermoplastic polyurethanes based on aliphatic diisocyanates nad polycarbonate diol. J Elastom Plast doi:10.1177/0095244316639633
15. Chen PH, Yang YF, Lee DK et al (2007) Synthesis and properties of transparent thermoplastic segmented polyurethanes. Adv Polym Technol 26(1):33–40
16. Hepburn C (1992) Trends in polyurethane elastomer technology. Iran J Polym Sci Technol 1:84–110
17. Sonnenschein MF, Rondan N, Wendt BL, Cox JM (2004) Synthesis of transparent thermoplastic polyurethane elastomers. J Polym Sci A Polym Chem 42:271–278
18. Lee DK, Tsai HB, Tsai RS, Chen PH (2007) Preparation and properties of transparent thermoplastic segmented polyurethanes derived from different polyols. Polym Eng Sci 47:695–701
19. Choi T, Weksler J, Padsalgikar A, Runt J (2011) Novel hard-block polyurethanes with high strength and transparency for biomedical applications. J Biomat Sci 22:973–980
20. Rogulska M, Kultys A (2016) Aliphatic polycarbonate-based thermoplastic polyurethane elastomers containing diphenyl sulfide units. J Therm Anal Calorim 126:225–243
21. Rogulska M, Kultys A, Lubczak J (2015) New thermoplastic polyurethane elastomers based on aliphatic–aromatic chain extenders with different content of sulfur atoms. J Therm Anal Calorim 121:397–410
22. Rogulska M, Kultys A, Olszewska E (2013) New thermoplastic poly(thiourethane-urethane) elastomers based on hexane-1,6-diyl diisocyanate (HDI). J Therm Anal Calorim 114:903–916

23. Kultys A, Puszka A (2013) New thermoplastic polyurethane elastomers based on sulfur-containing chain extenders. Pol J Chem Technol 15:1–6
24. Kultys A, Puszka A (2014) Transparent poly(thiourethane-urethane)s based on dithiol chain extender. Synthesis and characterization. J Therm Anal Calorim 117:1427–1439
25. Rogulska M, Kultys A, Puszka A (2016) New thermoplastic poly(carbonate-urethane)s based on chain extenders with sulfur atoms. Chem Pap doi:10.1007/s11696-016-0112-5
26. Puszka A, Kultys A (2017) The influence of soft segments on some properties of new transparent segmented polyurethanes. Polym Adv Technol. doi:10.1002/pat
27. Penczek S, Frisch KC, Szczepaniak B, Rudnik E (1993) Synthesis and properties of liquid crystalline polyurethanes. J Polym Sci A Polym Chem 31:1211–1220
28. Gorna K, Polowinski S, Gogolewski S (2002) Synthesis and characterization of biodegradable poly(ε-caprolactone urethane)s. I. Effect of the polyol molecular weight, catalyst, and chain extender on the molecular and physical characteristics. J Polym Sci A Polym Chem 40:156–170
29. Gunatillake PA, Meijs GF, Mccarthy SJ, Adhikari R, Sherriff N (1998) Synthesis and characterization of a series of poly(alkylene carbonate) macrodiols and the effect of their structure on the properties of polyurethanes. J Appl Polym Sci 69:1621–1633
30. Spirkova M, Poreba R, Pavlicevic J, Kobera L, Baldrian J, Pekarek M (2012) Aliphatic polycarbonate-based polyurethane elastomers and nanocomposites. I. The influence of hard-segment content and macrodiol-constitution on bottom-up self-assembly. J Appl Polym Sci 126:1016–1030
31. Costa L, Luda MP, Cameron GG, Qureshi MY (2000) The thermal and thermo-oxidative degradation of poly(tetrahydrofuran) and its complexes with LiBr and LiI. Polym Degrad Stabil 67:527–533
32. Li XG, Huang MR, Bai H, Yang YL (2002) High-resolution thermogravimetry of poly(phenylene-sulfide) film under four atmospheres. J Appl Polym Sci 83:1940–1946
33. Chattopadhyay DK, Webster DC (2009) Thermal stability and flame retardancy of polyurethanes. Prog Polym Sci 34:1068–1133
34. Li SF, Zhi J, Yuan KJ, Yu SQ, Chow WK (2006) Studies on the thermal behavior of polyurethanes. Polym Plast Technol 45:95–108
35. The website http://www.matweb.com. Accessed 1 Feb 2017